

5

The Tetranuclear Copper-Sulfide Center of Nitrous Oxide Reductase

Sofia R. Pauleta,^{1} Marta S. P. Carepo,² Isabel Moura²*

¹ Microbial Stress Lab, UCIBIO, REQUIMTE, Departamento de Química, Faculdade de Ciências e Tecnologia, Universidade Nova de Lisboa, PT-2829-516 Caparica, Portugal
<srp@fct.unl.pt>

² Biological Chemistry Lab, LAQV, REQUIMTE, Departamento de Química, Faculdade de Ciências e Tecnologia, Universidade Nova de Lisboa, PT-2829-516 Caparica, Portugal
<marta.carepo@fct.unl.pt>
<isabelmoura@fct.unl.pt>

*SRP planned and wrote the manuscript, with contributions from MSPC and IM.

ABSTRACT

1. INTRODUCTION
2. NITROUS OXIDE
 - 2.1. Properties and Reactions
 - 2.2. Sources of Nitrous Oxide
3. NITROUS OXIDE REDUCTASE
 - 3.1. Clade I and Clade II of Nitrous Oxide Reductase
 - 3.2. Structure, Biochemical and Catalytic Properties of Nitrous Oxide Reductase
4. THE CATALYTIC CuZ CENTER
 - 4.1. Structure of the CuZ Center

Metal Ions in Life Sciences, Volume 20, Guest Editors: Martha E. Sosa Torres and Peter M. H. Kroneck
Series Editors: Astrid Sigel, Eva Freisinger, and Roland K. O. Sigel
© Walter de Gruyter GmbH, Berlin, Germany 2020, www.mils-WdG.com
<https://doi ...>

Met. Ions Life Sci. **2020**, *20*, ...–...

- 4.2. Redox and Spectroscopic Properties of CuZ(4Cu1S) and CuZ(4Cu2S)
 - 4.3. Activation of the CuZ Center and Binding of Nitrous Oxide
 - 4.4. Catalytic Cycle of CuZ(4Cu1S)
 - 4.5. CuZ Center Assembly
5. GENERAL CONCLUSIONS AND FUTURE PERSPECTIVES

ACKNOWLEDGMENTS

ABBREVIATIONS AND DEFINITIONS

REFERENCES

Abstract: Nitrous oxide reductase catalyzes the reduction of nitrous oxide (N_2O) to dinitrogen (N_2) and water at a catalytic tetranuclear copper sulfide center, named CuZ, overcoming the high activation energy of this reaction. In this center each Cu atom is coordinated by two imidazole rings of histidine side-chains, with the exception of one named Cu_{IV} . This enzyme has been isolated with CuZ in two forms CuZ(4Cu1S) and CuZ(4Cu2S), which differ in the Cu_{I} - Cu_{IV} bridging ligand, leading to considerable differences in their spectroscopic and catalytic properties. The Cu atoms in CuZ(4Cu1S) can be reduced to the $[\text{4Cu}^{1+}]$ oxidation state, and its catalytic properties are compatible with the nitrous oxide reduction rates of whole cells, while in CuZ(4Cu2S) they can only be reduced to the $[\text{1Cu}^{2+}\text{-3Cu}^{1+}]$ oxidation state, which has a very low turnover number. The catalytic cycle of this enzyme has been explored and one of the intermediates, CuZ^0 , has recently been identified and shown to be in the $[\text{1Cu}^{2+}\text{-3Cu}^{1+}]$ oxidation state. Contrary to CuZ(4Cu2S), CuZ^0 is rapidly reduced intramolecularly by the electron transferring center of the enzyme, CuA, to $[\text{4Cu}^{1+}]$ by a physiologically relevant redox partner.

The three-dimensional structure of nitrous oxide reductase with the CuZ center either as CuZ(4Cu1S) or as CuZ(4Cu2S) shows that it is a unique functional dimer, with the CuZ of one subunit receiving electrons from CuA of the other subunit. The complex nature of this center has posed some questions relative to its assembly, which are only partially answered, as well as to which is the active form of CuZ *in vivo*.

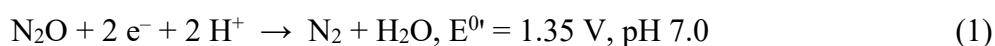
The structural, spectroscopic, and catalytic features of the two forms of CuZ will be

addressed here, as well as its assembly. The understanding of its catalytic features, activation and assembly is essential to develop strategies to decrease the release of nitrous oxide to the atmosphere and to reduce its concentration in the stratosphere, as well as to serve as inspiration to synthetic inorganic chemists to develop new models of this peculiar and challenging copper sulfide center.

Keywords: activation · biogenesis · catalytic mechanism · CuZ center · denitrification · greenhouse gas · nitrous oxide · nitrous oxide reductase

1. INTRODUCTION

Nitrous oxide (N₂O) is a powerful greenhouse gas with a major impact on global warming due to its long lifetime in the atmosphere, global warming potential (300 times higher than CO₂), and implications on the ozone layer depletion occurring in the stratosphere [1-6]. Nitrous oxide reductase (N₂OR) is the enzyme that catalyzes the reduction of N₂O to N₂ and water (Eq. (1)), transforming a powerful oxidant in two inert molecules, and overcoming a high energetic barrier that is associated with this chemical reaction [7, 8].



The active center of N₂OR is a tetranuclear copper center, CuZ, that is quite unique and complex not only in its geometry but also in its spectroscopic and catalytic properties [9, 10]. The complexity associated with CuZ is also due to the presence of a μ₄-sulfide ligand bridging the four copper atoms and to the nature of another ligand bridging Cu_I and Cu_{IV}, either a solvent derived ligand on an “open” edge, or a second sulfide (S²⁻). The binding of this sulfur ligand and its implications towards activity is still a matter of controversy and contributes to the uncertainty that is still associated with the catalytic mechanism proposed so far. Therefore, although the structure, spectroscopic, and catalytic properties of CuZ have been extensively studied there are several aspects of its activation, structure *in vivo*, and assembly that remain to be answered. Some of these aspects will be discussed here.

The uniqueness of the CuZ arrangement in Nature is even more puzzling since it is known that there is no need for tetranuclearity to obtain N₂O reduction, as binuclear copper model compounds have been shown to present activity towards N₂O [11]. Furthermore, contrary to other known enzymes able to catalyze reactions involving gases, such as hydrogenase, nitrogenase, CO dehydrogenase or even nitrite reductases, that show versatility towards the transition metals present in their active center to achieve catalysis [12-16], in the case of N₂OR this is not observed, and the CuZ center is the only known metal center among these enzymes found so far in Nature [17]. The specificity presented by the N₂OR active center must therefore be related with the properties and reactivity of N₂O that will be briefly discussed in Section 2.1.

2. NITROUS OXIDE

2.1. Properties and Reactions

N₂O reduction to N₂ is a highly exergonic reaction, with a ΔG° of -339.5 kJ/mol [18], however, it has a high energetic activation barrier of 250 kJ/mol [19] due to the electronic delocalization that stabilizes the molecule and because it corresponds to a spin-forbidden process [7]. N₂O has a dipole moment of 0.166 Debye, with double bond distances shorter than average, which are 1.128 Å and 1.184 Å, for N–N and N–O, respectively [7, 8]. The high reduction potential observed catalogues N₂O as a powerful oxidant and in Nature only N₂OR is able to overcome this activation barrier reducing this gas to the inert N₂ and water.

The atmospheric concentration of N₂O increased 22 % compared with the values estimated for the pre-industrial era, and in 2017 was approximately 330 ppb, corresponding to an increase of 0.25 % each year [5, 20, 21]. The photolytic action of sunlight in the stratosphere promotes N₂O decomposition to N₂ and O(¹D). A minor fraction of N₂O reacts with O(¹D) forming NO [5, 22, 23]. This reaction is an important source of reactive nitrogen species that will react with ozone accounting for the greenhouse effect of N₂O.

Due to the driving force to find efficient ways to decompose N₂O, hetero- and homogeneous catalysis using metal complexes have been described (some examples can be found in [24-26]), mainly involving non-transition metals, considering that N₂O is a weak ligand.

Model compounds that mimic the CuZ center are also being tested towards N₂O reduction and so far, there are already several multicopper clusters with the ability to react with this molecule. One example is the dissymmetric mixed-valent Cu(II)Cu(I) complex [2·(H₂O)(OTf)]¹⁺ (OTf = trifluoromethanesulfonate anion, CF₃SO₃⁻) published by Torelli and co-workers, containing OTf and H₂O as exchangeable ligands. This compound reduces N₂O to N₂, leading to a doubly bridged [Cu₂(μ-SR)(μ-OH)] complex as the final product [11]. Another example is the Cu¹⁺₂(μ-S) complex synthesized by Hillhouse and co-workers, {(IPr*)Cu}₂(μ-S) (IPr* = 1,3-bis(2,6-diphenylmethyl)-4-methylphenyl)imidazole-2-ylidene) [27]. This complex reacts with N₂O giving rise to a mixture of six compounds, with [(IPr*)Cu]₂(μ-SO₄), as the major product of the reaction, and it is suggested that the role of the tetranuclearity observed for CuZ is a way to protect the μ₄-sulfur ligand from oxidation or expulsion [28]. Tolman's group synthesized a localized mixed valent Cu(II)Cu(I)₂ cluster bridged by disulfide, [L₃Cu₃(μ₃-S₂)]X₂ (L = 1,4,7-trimethyl-triazacyclononane, X = O₃SCF₃⁻ or SbF₆⁻). The cluster reacts with N₂O to yield N₂, computational analysis implicates a transition state structure that features μ-1,1-bridging of N₂O via its O-atom to a [L₂Cu₂(μ-S₂)]⁺ fragment [29]. The first model compound for the μ-sulfido-tetracopper CuZ center, with the ability to reduce N₂O, is one in which two molecules of a reduced amidinate-supported [Cu₄(μ₄-S)] cluster are able to reduce N₂O, one cluster acting as an activator and the other as a reductant [30].

2.2 Sources of Nitrous Oxide

Several studies have shown that N₂O emissions can come from natural sources like oceans, forests and savannas, as well as from anthropogenic sources. The anthropogenic sources of N₂O are identified as the agricultural soils, mainly the production of forages and nitrogen-fixing crops, livestock manure, as well as manure used as fertilizers, fossil fuel combustion, adipic and nitric acid industrial production, waste incineration, biomass burning, and waste water treatment plants [31-35].

From 1970 to 2012 according to the Emission Database for Global Atmospheric Research (EDGAR), N₂O emission expressed in CO₂ equivalents increased in Asia Pacific, Sub-Saharan Africa, Latin America, and the Caribbean region, and decreased in the European Union and

North America. The decrease in N₂O emissions observed in both Europe and North America is mainly a result of a reduction in N₂O emissions from mobile combustion, as well as from adipic and nitric acid industrial production together with motor emission control technologies for on-road vehicles. Agriculture soils associated to nitrogen fertilizers remains one of the major sources of N₂O emissions around the world [34, 35].

Microbial metabolic activities associated with the nitrogen biogeochemical cycle are responsible for the direct release of N₂O, as well as for the anthropogenic release arising from agriculture due to the use of nitrogen fertilizers [36-38]. The nitrogen cycle has five major pathways: nitrification, denitrification, nitrogen fixation, anaerobic ammonium oxidation (Anammox) and dissimilatory nitrate reduction to ammonium (DNRA) [39] (Figure 1).

insert Figure 1 in color close to here (width: 12 cm)

The N₂O release is mainly associated with denitrification and nitrification, as well as with DNRA pathway, though in a lesser extent [39-43]. Denitrification, the process corresponding to anaerobic respiration of nitrate, accounts for the major release of N₂O, since this molecule is the last intermediate in the four-step reduction of nitrate to N₂, and it is the product of a reaction catalyzed by the enzyme NO reductase that is responsible for the reduction of NO to N₂O, forming the N–N bond [32]. Not all microorganisms can perform the complete denitrification [44-46], reducing N₂O to N₂ in a reaction catalyzed by N₂OR, due to either the absence of the gene encoding N₂OR, *nosZ* (Section 3.1.) [47, 48], or by environmental conditions associated with low pH [49-51], presence of dioxygen (O₂) [52-54], carbon dioxide (CO₂) [55, 56], or sulfide (S²⁻) [57].

In the nitrification pathway three types of microorganisms are involved: (i) the ammonium oxidizers that are responsible for the oxidation of ammonium (NH₄⁺) to nitrite (NO₂⁻), (ii) the nitrite oxidizers that oxidize nitrite to nitrate (NO₃⁻), and (iii) the complete ammonium oxidizers that perform all steps from the oxidation of ammonium to nitrate [39]. In the nitrification pathway, occurring under oxic conditions, N₂O is formed during the oxidation of hydroxylamine (NH₂OH), when nitrite is present in low concentrations, while ammonium exists in high concentrations [58, 59]. Formation of ammonium is accomplished through two different processes, the DNRA or the direct reduction of dinitrogen (N₂) to ammonium (nitrogen fixation).

The bacteria and archaea involved in these processes have nitrogenases and in this step N_2O is formed in small amounts concomitantly with ammonium when nitrate/nitrite is being reduced [42, 60, 61]. Recently, it was found that chemodenitrification processes can also contribute to the formation of N_2O , in which Fe(II) reacts with nitrite forming nitric oxide (NO), which can further react with Fe(II) forming N_2O [62] (Section 3.1).

3. NITROUS OXIDE REDUCTASE

N_2OR catalyzes the N_2O reduction to N_2 according to Equation (1). This reaction is the last step of the metabolic denitrification pathway (Section 2.2, Figure 1) and is used by some microorganisms to produce a proton-driven force for ATP synthesis, under anoxic conditions [63]. N_2OR is a copper enzyme containing two different metal centers: (i) the binuclear mixed-valent **CuA center** [64], that acts as the electron transferring center, and (ii) the catalytic center, CuZ. This is a unique catalytic tetranuclear copper sulfide center, tailored by Nature to overcome the high activation energy of N_2O reduction and is the subject of this chapter.

3.1. Clade I and Clade II of Nitrous Oxide Reductase

N_2OR is encoded in the genome by *nosZ*. The comparative analysis of sequenced genomes encoding N_2OR led to the division of these organisms into two clades according to the gene composition of the *nosZ* operon. In Figure 2, the gene organization of the *nosZ* operon for these two clades is presented for a representative microorganism of each clade.

insert Figure 2 in color close to here (landscape)

Clade I N_2OR s have been isolated from proteobacteria of the α -, β -, and γ -division [65], with most of these genomes also encoding genes for the other enzymes of the denitrification pathway. These N_2OR s have been extensively characterized and the majority of the spectroscopic, kinetic, and structural data reported in the literature have been acquired for the Clade I enzymes.

Clade II N_2OR s are not so well characterized and have been shown to be encoded in the

genome of some Gram-positive bacteria, such as *Geobacillus thermodenitrificans* and other *Bacillus* species, and in proteobacteria of the δ - and ϵ -division [66-68]. Contrary to Clade I, these microorganisms have been classified as canonical non-denitrifiers because the genes *nirK* and *nirS*, which encode the copper-type and cytochrome *cd*₁-type nitrite reductases (see Figure 1), respectively, associated with denitrification are absent from their genomes [18, 47, 60, 61].

Clade II N₂OR has only been isolated from *Wolinella succinogenes* [69], and it was shown to bind a *c*-type heme in an additional C-terminal domain. This feature is a unique trait of *W. succinogenes* N₂OR [69-74], as the analysis of the primary sequence of other members of Clade II does not reveal the presence of the canonical *c*-type heme binding motif, -C(X)₂₋₄CH-. Nevertheless, several physiological studies have been performed using *Dechloromonas aromatica* and *Anaeromyxobacter dehalogenans* [61, 62]. These organisms have been gaining interest as they can convert nitrite to N₂ by linking abiotic to biotic reactions, in a process that involves the abiotic reduction of nitrite by Fe(II), as mentioned in Section 2.2, generating N₂O, which is then reduced to N₂ by N₂OR [62]. Thus, although these organisms do not encode the canonical denitrifying genes, they should no longer be classified as non-denitrifiers.

One major difference between Clade I and Clade II N₂OR is the enzyme's affinity for N₂O, with Clade I N₂OR exhibiting a lower affinity (around 20 μ M) than Clade II N₂OR (0.1 μ M), though a higher reduction rate is observed for the former [61, 75]. Another feature that distinguishes the enzymes of these two clades is the signal peptide for protein transport to the periplasm in Gram-negative bacteria. Clade I N₂OR is transported to the periplasm by the twin-arginine translocation (Tat) system in the folded state, while Clade II N₂OR is transported through the secretory pathway (Sec) in the unfolded state. In fact, proteins that require *c*-type heme attachment are transported to the periplasm through this system, though this is not the case for all members of Clade II. The reasoning for this difference is still unknown. Moreover, Clade II N₂ORs from Gram-negative bacteria are predicted to be membrane-associated, but none of these enzymes has yet been isolated.

Besides these differences, Clade I and Clade II N₂ORs also differ in the genes that constitute their *nosZ* operons. The genes proposed to be involved in CuZ center assembly (*nosDFYL*) (Section 4.5) are present in both clades, and there are others that differ from each

clade. The Clade II *nosZ* operon has two genes, *nosHG*, homologues to the ones encoding the quinol dehydrogenase NapHG [76], and two other encoding *c*-type cytochromes, which together are proposed to compose the electron transfer chain from menaquinol to N₂OR [69, 77] (Figure 2B). In the case of Clade I, *nosR* encodes an Fe-S protein with a periplasmic FMN binding domain [78, 79], NosR. This protein has been proposed to play a role in maintaining N₂OR in an active state and/or to be part of the electron transfer chain from the quinol pool to N₂OR [18, 78, 79] (Figure 2A). Another gene that is associated with the *nosZ* operon of Clade I N₂OR α -proteobacteria is *nosX*, which encodes a flavoprotein belonging to the ApbE protein family [80]. This protein was shown to be involved in the maturation of NosR by donating its FAD group [79], and explains why a *nosXnirX Paracoccus denitrificans* mutant strain was not able to reduce N₂O [80]. In the other Clade I microorganisms this role is played by a protein of the same family but its gene is usually distantly located in the genome from *the nosZ* operon [75, 79].

3.2. Structure, Biochemical and Catalytic Properties of Nitrous Oxide Reductase

Clade I N₂ORs have been isolated from different species and extensively characterized with their structure determined in different oxidation states, in the presence of iodide (Figure 3) and of N₂O [81-84]. These enzymes have also been studied using different spectroscopic techniques, and its kinetic parameters have been determined using either artificial or putative physiological electron donors. On the other hand, the N₂OR from *W. succinogenes* is the only Clade II enzyme isolated so far [70] and its structure is not yet known (only a model structure was proposed considering that this enzyme could be regarded as an electron transfer complex between Clade I N₂OR and a small electron transfer protein [85]).

The first report of a Clade I N₂OR dates back to 1972, when a copper enzyme was purified from *Alcaligenes faecalis* [86], but its catalytic activity was only discovered 10 years after for a similar protein isolated from *Pseudomonas stutzeri* [87]. Since then, there have been several reports on its purification from denitrifying microorganisms, with the more extensively studied enzymes being the ones isolated from *P. denitrificans*, *P. stutzeri*, and *Marinobacter hydrocarbonoclasticus*. These are periplasmic dimeric enzymes that bind 12 copper atoms per dimer, arranged in two multicopper centers: a binuclear Cu_A electron transfer center and a

tetranuclear copper sulfide center, CuZ, the active center at which N₂O binds and its reduction occurs.

The analysis of the *Clade I P. denitrificans* N₂OR primary sequence together with its X-ray structure revealed that these two copper centers are organized in two different domains of the enzyme: the N-terminal domain has a β -propeller structure with seven blades (Figure 3A), in the center of which the CuZ center is inserted, while the CuA center binds in the loop region between the β 8 and β 9 strands of the β -barrel C-terminal domain [82]. The two centers in the monomer are 40 Å apart but only at 10 Å, when considering different monomers (head-to-tail arrangement). Thus, the structural arrangement of N₂OR results in a functional dimer since the electron transfer has to occur between CuA and CuZ located in different monomers (Figure 3). The CuA center is very similar to the CuA centers present in cytochrome *c* oxidase [88] and quinol CuA nitric oxide reductase [89]. It is a binuclear copper center with two bridging cysteines binding the two copper atoms, through their S γ atom, with the other ligands being two N ϵ 2 atoms of the imidazole ring of two histidines, the S δ atom of a methionine and the carbonyl of a tryptophan residue. The properties of CuA center will not be further addressed here, as they are the focus of chapter 4 in this book [64].

insert Figure 3 in color close to here (width: 11 cm)

The specific activity of Clade I N₂OR isolated from different organisms has been reported to range from 1 and 10 $\mu\text{mol of N}_2\text{O min}^{-1}\text{mg}^{-1}$ N₂OR [90-94], while the one of Clade II *W. succinogenes* N₂OR is 160 $\mu\text{mol of N}_2\text{O min}^{-1}\text{mg}^{-1}$ N₂OR [70, 73]. The electrons required for the catalytic reduction of N₂O can be donated by small periplasmic *c*-type cytochromes [95-97] or type 1 copper proteins [95, 98], depending on the microorganism, and mitochondrial cytochrome *c* has also been used in some cases as a non-physiological electron donor [99-101]. Besides the *in vitro* assays, whole cell studies have shown that during N₂O reduction oxidation of a cytochrome in the case of *Rhodobacter capsulatus*, *Rhodobacter sphaeroides*, and *P. denitrificans* [96, 102] occurs, and that a *R. capsulatus* cytochrome *c*₂ knock-out strain was unable to reduce N₂O [97]. This strengthens the hypothesis that small electron transfer proteins are involved in the electron transfer pathway during N₂O reduction. Nevertheless, the involvement of these small electron donor proteins does not exclude that *in vivo* there are other

proteins also involved in the electron transfer chain (Figure 2), such as NosR. This hypothesis has been strengthened by the observation that in *Pseudomonas aeruginosa* the denitrification enzymes form a supramolecular complex that includes also NosR [103, 104].

4. THE CATALYTIC CuZ CENTER

4.1. Structure of the CuZ Center

The catalytic center of N₂OR, “CuZ”, being a tetranuclear copper center bridged by a sulfur atom, has only been observed in N₂OR so far, in contrast to CuA [105, 106]. Its nuclearity foresees that five different oxidation states can be reached in this center (Scheme 1), but only three have been observed by spectroscopic techniques so far: [2Cu²⁺-2Cu¹⁺], [1Cu²⁺-3Cu¹⁺] and [4Cu¹⁺]. The first two were detected in isolated N₂ORs, while the later can only be obtained *in vitro* through a prolonged incubation with reduced viologens, as will be discussed in Section 4.3. In addition, the CuZ center can be observed in either of the forms, CuZ(4Cu1S) or CuZ(4Cu2S), that have different coordination spheres, as well as different spectroscopic, redox, and kinetic properties.

insert Scheme 1 here (width: 8 cm)

It is important to mention that N₂OR has never been isolated with the CuZ center in a single form, but usually the preparations are richer in either CuZ(4Cu2S), when isolated under anoxic conditions [93], or in CuZ(4Cu1S) when oxic conditions have been used, or the cells had been stored for a longer time at low temperature prior to enzyme isolation [93, 107].

The tetranuclear core structure of the CuZ was revealed for the first time when the X-ray structure of *M. hydrocarbonoclasticus* N₂OR together with the one of *P. denitrificans* N₂OR, both with the CuZ center mainly as CuZ(4Cu1S), was reported [81, 82]. The CuZ center is a tetranuclear μ_4 -sulfide-bridged copper center, adopting a distorted tetrahedral geometry. The Cu_I, Cu_{II}, and Cu_{III} atoms are each coordinated by two histidines, while Cu_{IV} is coordinated by only one (Figure 4). These copper atoms are coordinated by either N ϵ 2 (His80, His128, His270, His325, His376) or N δ 1 (His79 and His437) of the histidine imidazole ring (numbering of the

residues according to the primary sequence of *P. denitrificans* N₂OR) and there is also a solvent-derived molecule bridging Cu_I and Cu_{IV} (Figure 3B). These histidine residues are located in the blades (His79, His80, His128, His325 and His376) or in the top (His270 and His437) of the β -propeller N-terminal domain [81-84].

insert Figure 4 in color close to here (width: 12 cm)

The structure of CuZ(4Cu2S) in the [2Cu²⁺-2Cu¹⁺] oxidation state was reported 10 years later for *P. stutzeri* N₂OR, isolated under anoxic conditions [84], and revealed a second sulfur atom bridging Cu_I and Cu_{IV} instead of a solvent-derived molecule [84] (Figure 3B).

The structural difference between CuZ(4Cu1S) and CuZ(4Cu2S) makes their redox, spectroscopic, and kinetic properties to be different, as discussed in the following Sections.

4.2. Redox and Spectroscopic Properties of CuZ(4Cu1S) and CuZ(4Cu2S)

In the case of CuZ(4Cu1S), the oxidation state of the four copper atoms was determined by Cu K-edge X-ray absorption spectroscopy to be [1Cu²⁺-3Cu¹⁺] [108]. Several spectroscopic techniques have been used to characterize this center [108-112], showing that it exhibits an absorption maximum at 640 nm ($\epsilon_{640\text{nm}} \approx 3.5 \text{ mM}^{-1}\text{cm}^{-1}$ per monomer) and a broad axial electron paramagnetic resonance (EPR) signal ($g_{\parallel} = 2.16$ and $g_{\perp} \approx 2.04$) with poorly resolved hyperfine-split lines in the parallel region [107, 108, 113-117] (Table 1). Theoretical calculations using the structure of this center were instrumental to interpret the spectroscopic data and show that the spin density, $S_{\text{Total}} = \frac{1}{2}$, is mainly delocalized over Cu_I (26 %) and Cu_{IV} (12 %), with 26 % on the bridging sulfur [118]. The nature of the Cu_I-Cu_{IV} edge was identified examining the density functional theory (DFT) models of CuZ(4Cu1S) with different edge ligands (bridging H₂O, H₂O bound to Cu_I, bridging OH⁻, or OH⁻ bound to Cu_{IV} and H-bonded to a protonated lysine residue) [110-112]. The data showed that the spectroscopic properties of CuZ(4Cu1S) were better explained considering a model in which a OH⁻ ligand occupies the Cu_I-Cu_{IV} edge, closer to Cu_I (2.00 Å) than to Cu_{IV} (2.09 Å), and in which Lys397 and Glu435 are H-bonded to each other [112, 119] (numbering according to *P. denitrificans* N₂OR amino acid sequence).

CuZ(4Cu1S), in the $[1\text{Cu}^{2+}\text{-}3\text{Cu}^{1+}]$ oxidation state, cannot be oxidized by potassium ferricyanide and it is also not easily reduced *in vitro* by just sodium dithionite (-471 mV versus SHE at pH 7.0 [120]). Nevertheless, the $[4\text{Cu}^{1+}]$ oxidation state is observed after a prolonged incubation with reduced methyl or benzyl viologen (Table 1), but the redox potential of the $[1\text{Cu}^{2+}\text{-}3\text{Cu}^{1+}]/[4\text{Cu}^{1+}]$ pair could not be determined by potentiometry as it is an irreversible process [121].

insert Table 1 close to here (landscape)

Contrary to CuZ(4Cu1S), CuZ(4Cu2S) can exist in either the $[2\text{Cu}^{2+}\text{-}2\text{Cu}^{1+}]$ or the $[1\text{Cu}^{2+}\text{-}3\text{Cu}^{1+}]$ oxidation state, in an equilibrium that has a reduction potential of $+60$ mV, at pH 7.5 [93], but the $[4\text{Cu}^{1+}]$ oxidation state has never been observed so far, *not even in vitro*.

In the $[2\text{Cu}^{2+}\text{-}2\text{Cu}^{1+}]$ oxidation state, CuZ(4Cu2S) is characterized by an absorption maximum at 550 nm ($\epsilon_{550\text{nm}} \approx 5.0$ $\text{mM}^{-1}\text{cm}^{-1}$ per monomer), while the $[1\text{Cu}^{2+}\text{-}3\text{Cu}^{1+}]$ oxidation state exhibits an absorption maximum around 670 nm ($\epsilon_{670\text{nm}}$ $3.0\text{--}4.4$ $\text{mM}^{-1}\text{cm}^{-1}$ per monomer) (Table 1) [93, 94, 119]. Of these two oxidation states, the only EPR-active state of CuZ(4Cu2S) is $[1\text{Cu}^{2+}\text{-}3\text{Cu}^{1+}]$, since magnetic circular dichroism (MCD) showed that the $[2\text{Cu}^{2+}\text{-}2\text{Cu}^{1+}]$ oxidation state was diamagnetic. The EPR spectrum of CuZ(4Cu2S) in the $[1\text{Cu}^{2+}\text{-}3\text{Cu}^{1+}]$ oxidation state exhibits an axial signal ($g_{\parallel} > g_{\perp} > 2.0$), with five evenly spaced hyperfine lines in the g_{\parallel} region [119]. This signal was interpreted considering three identical $^{63,65}\text{Cu}$ hyperfine coupling constants of 5.6 mT [119] (Table 1), with the spin density being distributed over Cu_I (17 %), Cu_{II} (11 %) and Cu_{IV} (10 %), with the remaining spin density being over μ_4 -sulfide (34 %), $\mu_2\text{-SH}^-$ (16 %) and Cu_{III} (6 %) [119].

The protonation state of the bridging sulfur ligand was assessed in the two oxidation states by studying the pH profile of the CuZ(4Cu2S) resonance Raman spectra in combination with DFT calculations. The observation of D_2O -isotope sensitive vibration modes, identified as S-H bending modes, indicated that the $\text{Cu}_I\text{-Cu}_{IV}$ edge is a sulfide ($\mu_2\text{S}^{2-}$), with a $\text{p}K_a \leq 3$, in the $[2\text{Cu}^{2+}\text{-}2\text{Cu}^{1+}]$ oxidation state, and a hydrosulfide ($\mu_2\text{SH}^-$) with a $\text{p}K_a \geq 11$ in the $[1\text{Cu}^{2+}\text{-}3\text{Cu}^{1+}]$ oxidation state [119] (Table 1).

4.3. Activation of the CuZ Center and Binding of Nitrous Oxide

As mentioned in Section 3.2., the specific activity of isolated Clade I N₂OR is very low (1–10 μmol of N₂O min⁻¹mg⁻¹ N₂OR [90-94]), and does not explain the N₂O reduction rates observed for whole cells or crude cell extracts (48–72 μmol of N₂O min⁻¹mg⁻¹ N₂OR [75, 90, 127]). This observation led to the hypothesis that this enzyme requires activation and is isolated in an unready state [10]. On the contrary, the specific activity of Clade II *W. succinogenes* N₂OR was reported to be 160 μmol of N₂O min⁻¹mg⁻¹ N₂OR [70, 73], which might mean that Clade II N₂ORs are isolated in a ready state. However, kinetic studies on other enzymes from this clade are needed to confirm this hypothesis.

The specific activity of Clade I N₂ORs with CuZ(4Cu1S) increases during incubation with reduced methyl viologen and reaches a maximum value of 200 μmol of N₂O min⁻¹mg⁻¹ N₂OR after 3–5 h, in the case of *M. hydrocarbonoclasticus* N₂OR [99, 119]. During this time, by monitoring the EPR signal of the enzyme, it could be shown that the activation step is the reduction of CuZ(4Cu1S) from the [1Cu²⁺-3Cu¹⁺] to the [4Cu¹⁺] oxidation state [124, 128], as the EPR signal decreases, evidencing the formation of a diamagnetic species. The rate constant of this activation process was estimated to be $1.2 \times 10^{-3} \text{ s}^{-1}$ at pH 7.0 for *M. hydrocarbonoclasticus* N₂OR [124], indicating that it is too slow to be part of the catalytic cycle of the enzyme with a turnover number of 321 s⁻¹ (turnover number of *M. hydrocarbonoclasticus* N₂OR with CuZ(4Cu1S) in the [4Cu¹⁺] oxidation state) (Table 1) [123, 128].

In the case of CuZ(4Cu2S), the only catalytically competent oxidation state is [1Cu²⁺-3Cu¹⁺], but its turnover number is much lower, 0.6 h⁻¹ [123] (Table 1). Thus, it can be proposed that *in vivo* an activation step must occur prior to catalysis and that while N₂O is available, N₂OR is kept active by (a) still unidentified protein(s), avoiding inactivation after each catalytic cycle.

In fact, there has been a debate between the different research groups studying N₂OR as whether the [4Cu¹⁺] oxidation state is ever attained *in vivo*. Although, this question has not yet been answered, the analysis of the kinetic parameters of N₂OR with CuZ(4Cu1S) in the [4Cu¹⁺] oxidation state together with the estimation of the reduction rates of whole cells can help to clarify this question. In the case of *M. hydrocarbonoclasticus* N₂OR, a V_{max} of 200 μmol of N₂O min⁻¹mg⁻¹ N₂OR and a K_M of 18 μM were estimated from the kinetic assays using reduced

methyl viologen as electron donor [99]. A similar affinity constant was determined for these cells in the reduction of exogenously added N₂O. Moreover, the estimated V_{max} for the isolated N₂OR explains the high N₂O-reduction rate observed for the cells growing in the presence of nitrate, when considering the yield of the enzyme purification [75]. Hence, these data corroborated the hypothesis that N₂OR with the CuZ center in the [4Cu¹⁺] oxidation state can be the ready state of this enzyme *in vivo*.

One other argument for CuZ(4Cu1S) being part of the catalytic cycle of the enzyme *in vivo* was the observation that iodide, a proposed inhibitor of N₂OR, binds to the CuZ center at the Cu_I-Cu_{IV} edge [83], where a solvent-derived molecule has been modeled in the structure of *Achromobacter cycloclastes* N₂OR with CuZ(4Cu1S) in the [1Cu²⁺-3Cu¹⁺] oxidation state [81-83] (Figure 5). This observation was used to model the binding of N₂O to “CuZ” center by DFT calculations, with the μ-1,3-N₂O coordination at the Cu_I-Cu_{IV} edge of CuZ(4Cu1S) in the [4Cu¹⁺] oxidation state being found to be the most favorable binding mode for the substrate (Figure 5) [111, 117, 118, 124]. However, it can be argued that there has not been any other experimental evidence for the binding of the substrate to CuZ(4Cu1S). In an attempt to experimentally observe the binding of N₂O to CuZ(4Cu2S), the crystals of *P. stutzeri* N₂OR with CuZ(4Cu2S) in the [2Cu²⁺-2Cu¹⁺] oxidation state were pressurized with N₂O [84]. It was observed that the substrate was over the CuZ center [84], at a distance such that it cannot be considered to be coordinating any of the copper atoms. Moreover, it was later shown that in this oxidation state CuZ(4Cu2S) does not react with N₂O [123], so this structural rearrangement is not relevant for the catalytic cycle.

insert Figure 5 in color close to here (width: 12 cm)

In conclusion, even if CuZ(4Cu1S) is obtained when N₂OR is isolated under conditions that can be considered to damage its catalytic center (presence of dioxygen), this is the only form of the CuZ with high specific activity. One of the remaining questions to be answered is how CuZ(4Cu2S) is activated and whether this process involves the displacement of the μ₂-sulfur bridging ligand and whether NosR or another membrane-associated protein complex plays a role in the activation mechanism and catalytic activity of N₂OR.

4.4. Catalytic Cycle of CuZ(4Cu1S)

The catalytic cycle of CuZ(4Cu1S) has been proposed recently (Figure 6). The catalysis starts with the CuZ center in the fully reduced state, [4Cu¹⁺] (intermediate 1), reacting with the substrate, N₂O, to form intermediate 2. During this process, as mentioned in Section 4.3, N₂O binds with its terminal N to Cu_I in a linear configuration [118], and elongation of the N–O bond leads to the rearrangement of its structure, so that it binds at the Cu_I-Cu_{IV} edge in a μ-1,3-N₂O coordination forming a 139° N-N-O bond angle. In this intermediate 2, the oxygen atom is H-bonded to the protonated amino group of Lys397 [124, 129], but this intermediate has not yet been isolated.

insert Figure 6 close to here (width: 12 cm)

The release of N₂ requires two electrons that will be transferred, via Cu_{IV}, from the fully reduced CuZ(4Cu1S) [4Cu¹⁺], in a proton-coupled process, with all four copper atoms of CuZ(4Cu1S) being involved [118]. The cleavage of the N–O bond requires one electron, with one proton being simultaneously transferred from Lys397 to the oxygen, that becomes coordinated to Cu_{IV} as a hydroxide. The second electron is transferred, cleaving the Cu_I-N bond and leading to the release of N₂. Re-protonation of Lys397, with a proton from the solvent, coupled with electron transfer from the CuA center leads to the formation of CuZ⁰, intermediate 3. In this intermediate, the protonated form of Lys397 is H-bonded to the hydroxide ligand of Cu_{IV}, and to Glu435 to stabilize the CuZ⁰ intermediate [118]. The catalytic cycle is closed by the rapid intramolecular electron transfer via the CuA center ($k_{IET} > 0.1 \text{ s}^{-1}$) [118] (Figure 6).

The first intermediate, CuZ(4Cu1S) in the [4Cu¹⁺] oxidation state, has all its copper atoms in a d¹⁰ configuration and thus it is spectroscopically silent, but upon stoichiometric reaction with N₂O the intermediate CuZ⁰ is observed. This species is characterized by an absorption maximum at 680 nm ($\epsilon_{680\text{nm}} \approx 2.0 \text{ mM}^{-1}\text{cm}^{-1}$) and it reacts rapidly with the substrate without further activation [118, 121], indicating that it is directly involved in the catalytic cycle of the enzyme. CuZ⁰ has *g* values similar to those observed for CuZ(4Cu1S) in the [1Cu²⁺-3Cu¹⁺] oxidation state: $g_{\parallel} = 2.177 > g_{\perp} = 2.05 > 2.0$ [121], with two equal ^{63,65}Cu hyperfine coupling constants ($A_{\parallel} = 4.2 \text{ mT}$) to account for the 6-line hyperfine pattern in the parallel region (Table 1). This means

that the total spin in CuZ^0 is equally distributed between Cu_I and Cu_{IV} , while as it was mentioned before in $\text{CuZ}(4\text{Cu1S})$ in the same oxidation state Cu_I has a higher spin density.

The analysis of resonance Raman and MCD spectroscopic data used to characterize CuZ^0 corroborated that the four copper atoms are in the $[\text{1Cu}^{2+}\text{-3Cu}^{1+}]$ oxidation state [118], and that Cu_I and Cu_{IV} have a different coordination sphere from the one in $\text{CuZ}(4\text{Cu1S})$ in the same oxidation state. On the basis of DFT calculations the most plausible structure is the one presented in Figure 6, with a hydroxo ligand terminally coordinating Cu_{IV} with a **H-bonded** to a protonated lysine [118]. Thus, in CuZ^0 there is no bridging ligand between Cu_I and Cu_{IV} .

CuZ^0 can be reduced intramolecularly by CuA *in vitro*, in an experiment using a more physiologically relevant electron donor than methyl viologen, sodium ascorbate (with a reduction potential of + 60 mV) [118]. These experiments showed that the intramolecular electron transfer rate constant is higher than 0.1 s^{-1} [118].

4.5. CuZ Center Assembly

The CuZ center is a complex metal center with four copper atoms bound to an inorganic sulfur and coordinated by the imidazole rings of seven histidine residues that are bound to the center of a seven-bladed β -propeller domain. Thus, it is not solvent-exposed as other copper centers and attempts to heterologously produce N_2OR in microorganisms that do not have the *nosZ* operon in their genome have failed [130]. This indicates that the assembly machinery of the CuZ center might be as complex as the ones of Fe-S or *c*-type heme-containing proteins.

The presence of conserved genes in the *nosZ* operons of both Clade I and Clade II N_2ORs (Figure 2), *nosDFYL*, [9] has led to the hypothesis that the encoded proteins could play a role in the activity or metal center assembly of these enzymes. The metal center assembly of N_2OR from **either clade** has not been extensively explored but it is proposed to occur in the periplasm of Gram-negative bacteria, to which the apo- N_2OR is transported either in the folded or unfolded state by the Tat or the Sec system, respectively (Section 3.1). In fact, the X-ray structure of Clade I *Shewanella denitrificans* apo- N_2OR has been reported [130]. In this structure, the two domains have a similar fold as in the holo- N_2OR , and in the absence of a structural Ca^{2+} ion the regions surrounding the copper centers show structural disorder. Notably, the binding of Ca^{2+} and

ordering of the protein backbone prevent further access to the two copper centers. Most likely, the polypeptide chain requires some flexibility for proper copper insertion.

In the case of the CuA center, it has been proposed that its assembly is dependent on the same molecular system as the one involved in the assembly of CuA in cytochrome *c* oxidase [131], while the CuZ center assembly follows a different route. One evidence that there is a different route for CuZ assembly is the fact that N₂OR purified from *P. stutzeri* mutant strains with *nosDFY* knocked out only presents spectroscopic features of CuA [115, 132]. A similar result was obtained when analyzing the spectroscopic properties of N₂OR isolated from a *Pseudomonas putida* strain expressing only *nosZnosR* [133].

The product of *nosDFY* has been proposed to form an ABC transporter used for sulfur mobilization, transport, and insertion into the CuZ [134, 135]. The cytoplasmic component, NosF, is proposed to hydrolyze ATP to transport sulfur in an energy-dependent manner across NosY. NosF has a “Walker A” motif in its primary sequence and other features of an ATPase [134, 136], with its activity being Mg²⁺-dependent with a *K_M* of 3 mM for the hydrolysis of ATP and 10 mM for GTP [136]. NosY is a six-span membrane protein proposed to form a pore connecting the cytoplasmic NosF with the periplasmic NosD [131]. NosD has not yet been isolated, but the analysis of its primary sequence proposes that it has two β-helical domains with 4/5 parallel β-helix repeats with homology to proteins belonging to the carbohydrate-binding and sugar hydrolase protein family [135].

NosL is a small periplasmic outer-membrane bound protein classified as a copper chaperone [137-139]. It has two homologous domains with a β-β-α-β topology and binds specifically Cu¹⁺ in a 1:1 stoichiometry [138, 140]. Although it was proposed that NosL was not essential for the CuZ center assembly [133, 141], its presence in the *P. aeruginosa* supramolecular complex involving N₂OR and other enzymes participating in the denitrification pathway [103, 104], contradicted those initial findings. Recent work by the team of A. J. Gates and N. E. Le Brun has shown that in fact NosL is a dedicated copper chaperon essential for CuZ assembly under certain environmental conditions, such as low copper concentrations [140].

In conclusion, little is known about N₂OR biogenesis. It is expected that in the near future a better characterization of the proteins proposed to be involved in CuA and CuZ center

assemblies will shed more light into this process, together with the isolation of the intermediate forms of N₂OR during this process. Moreover, it cannot be ruled out that more proteins and enzymes might be involved in this process, besides the ones mentioned here, considering the complex nature of N₂OR and in particular of the CuZ center.

5. GENERAL CONCLUSIONS AND FUTURE PERSPECTIVES

Due to the growing importance of N₂O emissions to global warming, the development of mitigation strategies is extremely important to control N₂O emissions. N₂OR catalyzes the reduction of N₂O to N₂ and studies characterizing the “CuZ” active center of this enzyme, together with environmental stresses able to inactivate N₂OR function or production, represent an important contribution for the design of successful strategies to control atmospheric N₂O release by anthropogenic and natural sources.

The high complexity associated with the CuZ of N₂OR cannot be separated from the large activation barrier needed to overcome N₂O reduction to generate N₂ and water. N₂OR is a functional dimer with a unique catalytic copper center that can be isolated in two different forms: CuZ(4Cu1S), and CuZ(4Cu2S). These two centers have different specific activities, with CuZ(4Cu2S) reacting with N₂O with a low turnover number (0.6 h⁻¹), only in the [1Cu²⁺-3Cu¹⁺] oxidation state, while CuZ(4Cu1S), with a high turnover number activity in the [4Cu¹⁺] oxidation state, is considered to be the catalytic form that explains the high N₂O reduction rate of whole cells. This reduced form of CuZ(4Cu1S) reacts stoichiometrically with N₂O to complete the catalytic cycle, and in the absence of reducing power an intermediate is formed, CuZ. This intermediate is in the [1Cu²⁺-3Cu¹⁺] oxidation state with a hydroxide binding to Cu_{IV}, that can be displaced by the substrate, when there are enough available electrons to continue the catalytic cycle.

In the future, the elucidation of the coordination sphere of CuZ(4Cu1S) in the [4Cu¹⁺] oxidation state and of CuZ⁰, will be instrumental to understand their high reactivity and point out changes in the positioning of residues that could be involved in electron transfer and/or in stabilizing *in vivo* the active state of “CuZ”. In fact, it is still unknown whether N₂OR requires

activation *in vivo* and how its active form is maintained. The isolation of N₂OR with CuZ(4Cu₂S), which has a low specific activity, raised the hypothesis that this could be a protective form of the enzyme when the substrate or electrons are not available. However, the mechanism to either remove the μ_2 -bridging sulfur, or to increase its specific activity is still unknown. There is the possibility that accessory proteins, such as NosR, could play a role in these processes, but this hypothesis requires experimental validation.

The biogenesis of N₂OR that involves the assembly of two metal centers, CuA and “CuZ” needs to be further explored. The CuA center being similar to the one present in cytochrome *c* oxidase, could be assembled using a similar pathway without the need for specific proteins, however, the same is not expected for the CuZ center. The assembly machinery of CuZ is proposed to be encoded in the *nosZ* operon, by *nosDFYL*, but only a few of these proteins have been characterized and their involvement in Cu or S assembly/transport/delivery remains to be identified.

The better and more complete understanding of the CuZ center activity and assembly will for sure be of use to design strategies to mitigate the concentration of N₂O in the stratosphere, as well as control its emissions from soils and water environments and have an impact on the climate change.

ACKNOWLEDGMENT

We would like to thank I. Cabrito, S. Dell’Acqua, C. Carreira, and E. Johnston, for their contribution for the work presented here. We would also like to acknowledge the contributions of J. J. G. de Moura, C. Cambillau, E. Solomon, and O. Einsle for the fruitful discussions and collaborative work during the past years.

The authors would like to thank Fundação para a Ciência e Tecnologia (FCT) for the financial support provided (PTDC/BIA-PRO/098882/2008 to SRP and PTDC/BBB-BQB/0129/2014 to IM and MSPC). This work was further supported by the Associate Laboratory for Green Chemistry- LAQV and Unidade de Ciências Biomoleculares Aplicadas-UCIBIO, which is financed by national funds from FCT/MCTES (UID/QUI/50006/2019 and UID/Multi/04378/2019, respectively). MSPC acknowledges FCT/MCTES for funding her

"Research Position" (signed with FCT NOVA in accordance with DL.57/2016 and Lei 57/2017).

ABBREVIATIONS AND DEFINITIONS

| | |
|-------------------|---|
| Anammox | anaerobic ammonium oxidation |
| ATP | adenosine 5'-triphosphate |
| DFT | density functional theory |
| DNRA | dissimilatory nitrate reduction to ammonium |
| EPR | electron paramagnetic resonance |
| FAD | flavin adenine dinucleotide |
| FMN | flavin mononucleotide |
| GTP | guanosine 5'-triphosphate |
| N ₂ OR | nitrous oxide reductase |
| MCD | magnetic circular dichroism |
| Sec | secretory pathway |
| SHE | standard hydrogen electrode |
| Tat | twin-arginine translocation |

REFERENCES

1. Climate Change 2007: The Physical Science Basis, **2007**, Cambridge University Press.
2. Climate Change 2014: Mitigation of Climate Change, **2014**, Cambridge University Press.
3. A. R. Mosier, *Biol. Fertil. Soils* **1998**, 27(3), 221-229.
4. M. J. Prather, *Science* **1998**, 279(5355), 1339-1341.
5. A. R. Ravishankara, J. S. Daniel, R. W. Portmann, *Science* **2009**, 326(5949), 123-125.
6. W. C. Troglor, *J. Chem. Educ.* **1995**, 72(11), 973-976.
7. G. A. Vaughan, P. B. Rupert, G. L. Hillhouse, *J. Am. Chem. Soc.* **1987**, 109(18), 5538-5539.
8. L. Pauling, *Proc. Natl. Acad. Sci. U.S.A.* **1932**, 18(7), 498-499.
9. S. R. Pauleta, S. Dell'Acqua, I. Moura, *Coord. Chem. Rev.* **2013**, 257(2), 332-349.

10. S. R. Pauleta, C. Carreira, I. Moura, in *Metalloenzymes in Denitrification: Applications and Environmental Impacts*, Eds I. Moura, J. J. G. Moura, S. R. Pauleta, L. Maia, RSC, Cambridge, **2017**, pp. 141-169.
11. C. Esmieu, M. Orio, S. Torelli, L. Le Pape, J. Pecaut, C. Lebrun, S. Menage, *Chem. Sci.* **2014**, 5(12), 4774-4784.
12. F. Mus, D. R. Colman, J. W. Peters, E. S. Boyd, *Free Radic. Biol. Med.* **2019**.
10.1016/j.freeradbiomed.2019.01.050.
13. J. W. Peters, G. J. Schut, E. S. Boyd, D. W. Mulder, E. M. Shepard, J. B. Broderick, P. W. King, M. W. Adams, *Biochim. Biophys. Acta* **2015**, 1853(6), 1350-1369.
14. J. H. Jeoung, J. Fessler, S. Goetzl, H. Dobbek, *Met. Ions Life Sci.* **2014**, 14, 37-69.
15. S. Horrell, D. Kekilli, R. W. Strange, M. A. Hough, *Metallomics* **2017**, 9(11), 1470-1482.
16. L. B. Maia, J. J. Moura, *J. Biol. Inorg. Chem.* **2015**, 20(2), 403-433.
17. S. R. Pauleta, M. S. P. Carepo, I. Moura, *Coord. Chem. Rev.* **2019**, 387, 436-449.
18. W. G. Zumft, P. M. Kroneck, *Adv. Microb. Physiol.* **2007**, 52, 107-227.
19. K. Jones, in *Comprehensive Inorganic Chemistry*, Eds J. C. Bailar, H. J. Emelöus, R. Nyholm, A. F. Trotman-Dickenson, Pergamon Press, Oxford, **1975**, pp. 147-388.
20. D. J. Wuebbles, *Science* **2009**, 326(5949), 56-57.
21. W. Ye, L. Bian, C. Wang, R. Zhu, X. Zheng, M. Ding, *J. Environ. Sci.* **2016**, 47, 193-200.
22. K. Lasseby, M. Harvey, *Water & Atmosphere* **2007**, 15(2), 10-11.
23. R. W. Portmann, J. S. Daniel, A. R. Ravishankara, *Philos. Trans. R. Soc. Lond. B Biol. Sci.* **2012**, 367(1593), 1256-1264.
24. A. Miyamoto, S. Baba, M. Mori, Y. Murakami, *J. Physic. Chem.* **1981**, 85(21), 3117-3122.
25. R. Zeng, M. Feller, Y. Ben-David, D. Milstein, *J. Am. Chem. Soc.* **2017**, 139(16), 5720-5723.
26. A. Dandekar, M. A. Vannice, *Appl. Catal. B* **1999**, 22(3), 179-200.
27. J. Zhai, A. S. Filatov, G. L. Hillhouse, M. D. Hopkins, *Chem. Sci.* **2016**, 7(1), 589-595.
28. S. Bagherzadeh, N. P. Mankad, *Chem. Commun. (Camb)* **2018**, 54(9), 1097-1100.
29. I. Bar-Nahum, A. K. Gupta, S. M. Huber, M. Z. Ertem, C. J. Cramer, W. B. Tolman, *J. Am. Chem. Soc.* **2009**, 131(8), 2812-2814.

30. B. J. Johnson, W. E. Antholine, S. V. Lindeman, M. J. Graham, N. P. Mankad, *J. Am. Chem. Soc.* **2016**, *138*(40), 13107-13110.
31. N. Gruber, J. N. Galloway, *Nature* **2008**, *451*(7176), 293-296.
32. J. N. Galloway, A. R. Townsend, J. W. Erisman, M. Bekunda, Z. Cai, J. R. Freney, L. A. Martinelli, S. P. Seitzinger, M. A. Sutton, *Science* **2008**, *320*(5878), 889-892.
33. J. N. Galloway, F. J. Dentener, D. G. Capone, E. W. Boyer, R. W. Howarth, S. P. Seitzinger, G. P. Asner, C. C. Cleveland, P. A. Green, E. A. Holland, D. M. Karl, A. F. Michaels, J. H. Porter, A. R. Townsend, C. J. Vöosmarty, *Biogeochemistry* **2004**, *70*(2), 153-226.
34. Inventory of U.S. Greenhouse Gas Emissions and Sinks: 1990–2017, **2019**, United States Environmental Protection Agency.
35. Annual European Union greenhouse gas inventory 1990–2014 and inventory report 2016, **2016**, European Environmental Agency.
36. T. J. Griffis, Z. Chen, J. M. Baker, J. D. Wood, D. B. Millet, X. Lee, R. T. Venterea, P. A. Turner, *Proc. Natl. Acad. Sci. U.S.A.* **2017**, *114*(45), 12081-12085.
37. I. Shcherbak, N. Millar, G. P. Robertson, *Proc. Natl. Acad. Sci. U.S.A.* **2014**, *111*(25), 9199-9204.
38. W. H. Schlesinger, *Proc. Natl. Acad. Sci. U.S.A.* **2009**, *106*(1), 203-208.
39. L. Y. Stein, M. G. Klotz, *Curr. Biol.* **2016**, *26*(3), R94-98.
40. L. Y. Stein, Y. L. Yung, *Annu. Rev. Earth and Planet. Sci.* **2003**, *31*(1), 329-356.
41. L. Y. Stein, M. G. Klotz, *Biochem. Soc. Trans.* **2011**, *39*(6), 1826-1831.
42. S. Hallin, L. Philippot, F. E. Löffler, R. A. Sanford, C. M. Jones, *Trends Microbiol.* **2018**, *26*(1), 43-55.
43. G. Braker, R. Conrad, *Adv. Appl. Microbiol.* **2011**, *75*, 33-70.
44. H. Shoun, S. Fushinobu, L. Jiang, S. W. Kim, T. Wakagi, *Philos. Trans. R. Soc. Lond. B Biol. Sci.* **2012**, *367*(1593), 1186-1194.
45. K. Maeda, A. Spor, V. Edel-Hermann, C. Heraud, M. C. Breuil, F. Bizouard, S. Toyoda, N. Yoshida, C. Steinberg, L. Philippot, *Sci. Rep.* **2015**, *5*, 9697.
46. S. A. Higgins, A. Welsh, L. H. Orellana, K. T. Konstantinidis, J. C. Chee-Sanford, R. A.

- Sanford, C. W. Schadt, F. E. Löffler, *Appl. Environ. Microbiol.* **2016**, 82(10), 2919-2928.
47. D. R. Graf, C. M. Jones, S. Hallin, *PLoS One* **2014**, 9(12), e114118.
48. L. Philippot, J. Andert, C. M. Jones, D. Bru, S. Hallin, *Global Change Biol.* **2010**, 17(3), 1497-1504.
49. B. Liu, P. T. Mørkved, A. Frostegård, L. R. Bakken, *FEMS Microbiol. Ecol.* **2010**, 72(3), 407-417.
50. R. N. Van Den Heuvel, S. E. Bakker, M. S. M. Jetten, M. M. Hefting, *Geobiology* **2011**, 9(3), 294-300.
51. L. Bergaust, Y. Mao, L. R. Bakken, A. Frostegård, *Appl. Environ. Microbiol.* **2010**, 76(19), 6387-6396.
52. P. Lycus, M. J. Soriano-Laguna, M. Kjos, D. J. Richardson, A. J. Gates, D. A. Milligan, A. Frostegard, L. Bergaust, L. R. Bakken, *Proc. Natl. Acad. Sci. U.S.A.* **2018**, 115(46), 11820-11825.
53. L. Bergaust, R. J. van Spanning, A. Frostegard, L. R. Bakken, *Microbiology* **2012**, 158(Pt 3), 826-834.
54. J. Hassan, Z. Qu, L. L. Bergaust, L. R. Bakken, *PLoS Comput. Biol.* **2016**, 12(1), e1004621.
55. R. Wan, Y. Chen, X. Zheng, Y. Su, M. Li, *Environ. Sci. Technol.* **2016**, 50(18), 9915-9922.
56. R. Wan, L. Wang, Y. Chen, X. Zheng, Y. Su, X. Tao, *Sci. Total Environ.* **2018**, 643, 1074-1083.
57. J. H. Park, H. S. Shin, I. S. Lee, J. H. Bae, *Environ. Technol.* **2002**, 23(1), 53-65.
58. R. Yu, M. J. Kampschreur, M. C. van Loosdrecht, K. Chandran, *Environ. Sci. Technol.* **2010**, 44(4), 1313-1319.
59. P. Wunderlin, J. Mohn, A. Joss, L. Emmenegger, H. Siegrist, *Water Res.* **2012**, 46(4), 1027-1037.
60. R. A. Sanford, D. D. Wagner, Q. Wu, J. C. Chee-Sanford, S. H. Thomas, C. Cruz-Garcia, G. Rodriguez, A. Massol-Deya, K. K. Krishnani, K. M. Ritalahti, S. Nissen, K. T. Konstantinidis, F. E. Löffler, *Proc. Natl. Acad. Sci. U.S.A.* **2012**, 109(48), 19709-19714.
61. S. Yoon, S. Nissen, D. Park, R. A. Sanford, F. E. Löffler, *Appl. Environ. Microbiol.* **2016**,

- 82(13), 3793-3800.
62. J. R. Onley, S. Ahsan, R. A. Sanford, F. E. Löffler, *Appl. Environ. Microbiol.* **2017**, 10.1128/AEM.01985-17.
 63. W. G. Zumft, *Microbiol. Molec. Biol. Rev.* **1997**, 61(4), 533-616.
 64. D. H. Murgida, A. J. Vila, Chapter 4 of this book.
 65. C. Carreira, S. R. Pauleta, I. Moura, *J. Inorg. Biochem.* **2017**, 177, 423-434.
 66. C. M. Jones, A. Welsh, I. N. Throback, P. Dorsch, L. R. Bakken, S. Hallin, *FEMS Microbiol. Ecol.* **2011**, 76(3), 541-552.
 67. D. Mania, K. Heylen, R. J. van Spanning, A. Frostegard, *Environ. Microbiol.* **2014**, 16(10), 3196-3210.
 68. D. Mania, K. Heylen, R. J. van Spanning, A. Frostegard, *Environ. Microbiol.* **2016**, 18(9), 2937-2950.
 69. J. Simon, O. Einsle, P. M. Kroneck, W. G. Zumft, *FEBS Lett.* **2004**, 569(1-3), 7-12.
 70. S. Teraguchi, T. C. Hollocher, *J. Biol. Chem.* **1989**, 264(4), 1972-1979.
 71. C. S. Zhang, T. C. Hollocher, A. F. Kolodziej, W. H. Orme-Johnson, *J. Biol. Chem.* **1991**, 266(4), 2199-2202.
 72. C. Zhang, A. M. Jones, T. C. Hollocher, *Biochem. Biophys. Res. Commun.* **1992**, 187(1), 135-139.
 73. C. S. Zhang, T. C. Hollocher, *Biochim. Biophys. Acta* **1993**, 1142, 253-261.
 74. M. Luckmann, D. Mania, M. Kern, L. R. Bakken, A. Frostegard, J. Simon, *Microbiology* **2014**, 160(Pt 8), 1749-1759.
 75. C. Carreira, O. Mestre, R. F. Nunes, I. Moura, S. R. Pauleta, *PeerJ* **2018**, 6, e5603, DOI: 5610.7717/peerj.5603.
 76. M. Kern, J. Simon, *Biochim. Biophys. Acta* **2009**, 1787(6), 646-656.
 77. S. Hein, S. Witt, J. Simon, *Environ. Microbiol.* **2017**, 19(12), 4913-4925.
 78. P. Wunsch, W. G. Zumft, *J. Bacteriol.* **2005**, 187(6), 1992-2001.
 79. L. Zhang, C. Trncik, S. L. A. Andrade, O. Einsle, *Biochim. Biophys. Acta* **2017**, 1858(2), 95-102.
 80. P. Wunsch, H. Korner, F. Neese, R. J. van Spanning, P. M. Kroneck, W. G. Zumft, *FEBS*

- Lett.* **2005**, 579(21), 4605-4609.
81. K. Brown, K. Djinovic-Carugo, T. Haltia, I. Cabrito, M. Saraste, J. J. G. Moura, I. Moura, M. Tegoni, C. Cambillau, *J. Biol. Chem.* **2000**, 275(52), 41133-41136.
 82. K. Brown, M. Tegoni, M. Prudêncio, A. S. Pereira, S. Besson, J. J. G. Moura, I. Moura, C. Cambillau, *Nat. Struct. Biol.* **2000**, 7(3), 191-195.
 83. K. Paraskevopoulos, S. V. Antonyuk, R. G. Sawers, R. R. Eady, S. S. Hasnain, *J. Mol. Biol.* **2006**, 362(1), 55-65.
 84. A. Pomowski, W. G. Zumft, P. M. Kroneck, O. Einsle, *Nature* **2011**, 477(7363), 234-237.
 85. S. Dell'acqua, I. Moura, J. J. Moura, S. R. Pauleta, *J. Biol. Inorg. Chem.* **2011**, 16(8), 1241-1254.
 86. T. Matsubara, H. Iwasaki, *J. Biochem.* **1972**, 71(4), 747-750.
 87. W. G. Zumft, T. Matsubara, *FEBS Lett.* **1982**, 148(1), 107-112.
 88. H. Beinert, *Eur. J. Biochem.* **1997**, 245(3), 521-532.
 89. Suharti, M. J. Strampraad, I. Schroder, S. de Vries, *Biochemistry* **2001**, 40(8), 2632-2639.
 90. C. L. Coyle, W. G. Zumft, P. M. Kroneck, H. Korner, W. Jakob, *Eur. J. Biochem.* **1985**, 153(3), 459-467.
 91. C. K. SooHoo, T. C. Hollocher, *J. Biol. Chem.* **1991**, 266(4), 2203-2209.
 92. S. Ferretti, J. G. Grossmann, S. S. Hasnain, R. R. Eady, B. E. Smith, *Eur. J. Biochem.* **1999**, 259(3), 651-659.
 93. T. Rasmussen, B. C. Berks, J. N. Butt, A. J. Thomson, *Biochem. J.* **2002**, 364(Pt 3), 807-815.
 94. S. Dell'Acqua, S. R. Pauleta, J. J. Moura, I. Moura, *Philos. Trans. R. Soc. Lond. B Biol. Sci.* **2012**, 367(1593), 1204-1212.
 95. B. C. Berks, D. Baratta, D. J. Richardson, S. J. Ferguson, *Eur. J. Biochem.* **1993**, 212(2), 467-476.
 96. M. Itoh, K. Matsuura, T. Satoh, *FEBS Lett.* **1989**, 251(1-2), 104-108.
 97. D. J. Richardson, L. C. Bell, A. G. McEwan, J. B. Jackson, S. J. Ferguson, *Eur. J. Biochem.* **1991**, 199(3), 677-683.
 98. J. W. B. Moir, S. J. Ferguson, *Microbiology* **1994**, 140(2), 389-397.

99. S. Dell'acqua, S. R. Pauleta, E. Monzani, A. S. Pereira, L. Casella, J. J. Moura, I. Moura, *Biochemistry* **2008**, *47*(41), 10852-10862.
100. K. Fujita, J. M. Chan, J. a. Bollinger, M. L. Alvarez, D. M. Dooley, *J. Inorg. Biochem.* **2007**, *101*(11-12), 1836-1844.
101. T. Rasmussen, T. Brittain, B. C. Berks, N. J. Watmough, A. J. Thomson, *Dalton Trans.* **2005**. 10.1039/b501846c(21), 3501-3506.
102. F. C. Boogerd, H. W. van Verseveld, A. H. Stouthamer, *FEBS Lett.* **1980**, *113*(2), 279-284.
103. J. M. Borrero-de Acuna, M. Rohde, J. Wissing, L. Jansch, M. Schobert, G. Molinari, K. N. Timmis, M. Jahn, D. Jahn, *J. Bacteriol.* **2016**, *198*(9), 1401-1413.
104. J. M. Borrero-de Acuna, K. N. Timmis, M. Jahn, D. Jahn, *Microb. Biotechnol.* **2017**, *10*(6), 1523-1534.
105. S. Yoshikawa, A. Shimada, K. Shinzawa-Itoh, *Met. Ions Life Sci.* **2015**, *15*, 89-130.
106. T. Tosha, Y. Shiro, *IUBMB Life* **2013**, *65*(3), 217-226.
107. M. Prudencio, A. S. Pereira, P. Tavares, S. Besson, I. Cabrito, K. Brown, B. Samyn, B. Devreese, J. Van Beeumen, F. Rusnak, G. Fauque, J. J. Moura, M. Tegoni, C. Cambillau, I. Moura, *Biochemistry* **2000**, *39*(14), 3899-3907.
108. P. Chen, S. DeBeer George, I. Cabrito, W. E. Antholine, J. J. Moura, I. Moura, B. Hedman, K. O. Hodgson, E. I. Solomon, *J. Am. Chem. Soc.* **2002**, *124*(5), 744-745.
109. M. L. Alvarez, J. Ai, W. Zumft, J. Sanders-Loehr, D. M. Dooley, *J. Am. Chem. Soc.* **2001**, *123*(4), 576-587.
110. P. Chen, I. Cabrito, J. J. G. Moura, I. Moura, E. I. Solomon, *J. Am. Chem. Soc.* **2002**, *124*(35), 10497-10507.
111. P. Chen, S. I. Gorelsky, S. Ghosh, E. I. Solomon, *Angew. Chem.* **2004**, *43*(32), 4132-4140.
112. S. Ghosh, S. I. Gorelsky, George, S. DeBeer, J. M. Chan, I. Cabrito, D. M. Dooley, J. J. G. Moura, I. Moura, E. I. Solomon, *J. Am. Chem. Soc.* **2007**, *129*(13), 3955-3965.
113. J. A. Farrar, A. J. Thomson, M. R. Cheesman, D. M. Dooley, W. G. Zumft, *FEBS Lett.* **1991**, *294*(1-2), 11-15.
114. V. S. Oganessian, T. Rasmussen, S. Fairhurst, A. J. Thomson, *Dalton Trans.* **2004**. 10.1039/b313913a(7), 996-1002.

115. D. M. Dooley, M. A. McGuirl, A. C. Rosenzweig, J. A. Landin, R. A. Scott, W. G. Zumft, F. Devlin, P. J. Stephens, *Inorg. Chem.* **1991**, *30*(15), 3006-3011.
116. J. A. Farrar, W. G. Zumft, A. J. Thomson, *Proc. Natl. Acad. Sci. U.S.A.* **1998**, *95*(17), 9891-9896.
117. E. I. Solomon, D. E. Heppner, E. M. Johnston, J. W. Ginsbach, J. Cirera, M. Qayyum, M. T. Kieber-Emmons, C. H. Kjaergaard, R. G. Hadt, L. Tian, *Chem. Rev.* **2014**, *114*(7), 3659-3853.
118. E. M. Johnston, C. Carreira, S. Dell'Acqua, S. G. Dey, S. R. Pauleta, I. Moura, E. I. Solomon, *J. Am. Chem. Soc.* **2017**, *139*(12), 4462-4476.
119. E. M. Johnston, S. Dell'Acqua, S. R. Pauleta, I. Moura, E. I. Solomon, *Chem. Sci.* **2015**, *6*(10), 5670-5679.
120. S. G. Mayhew, *Eur. J. Biochem.* **1978**, *85*(2), 535-547.
121. S. Dell'Acqua, S. R. Pauleta, P. M. P. de Sousa, E. Monzani, L. Casella, J. J. G. Moura, I. Moura, *J. Biol. Inorg. Chem.* **2010**, *15*(6), 967-976.
122. T. Rasmussen, B. C. Berks, J. Sanders-Loehr, D. M. Dooley, W. G. Zumft, A. J. Thomson, *Biochemistry* **2000**, *39*(42), 12753-12756.
123. E. M. Johnston, S. Dell'Acqua, S. Ramos, S. R. Pauleta, I. Moura, E. I. Solomon, *J. Am. Chem. Soc.* **2014**, *136*(2), 614-617.
124. S. Ghosh, S. I. Gorelsky, P. Chen, I. Cabrito, J. J. G. Moura, I. Moura, E. I. Solomon, *J. Am. Chem. Soc.* **2003**, *125*(51), 15708-15709.
125. K. Yamaguchi, A. Kawamura, H. Ogawa, S. Suzuki, *J. Biochem.* **2003**, *134*(6), 853-858.
126. S. W. Snyder, T. C. Hollocher, *J. Biol. Chem.* **1987**, *262*(14), 6515-6525.
127. H. Körner, K. Frunzke, K. Döhler, W. G. Zumft, *Arch. Microbiol.* **1987**, *148*(1), 20-24.
128. J. M. Chan, J. Bollinger, C. L. Grewell, D. M. Dooley, *J. Am. Chem. Soc.* **2004**, *126*(10), 3030-3031.
129. M. Z. Ertem, C. J. Cramer, F. Himo, P. E. Siegbahn, *J. Biol. Inorg. Chem.* **2012**, *17*(5), 687-698.
130. L. K. Schneider, O. Einsle, *Biochemistry* **2016**, *55*(10), 1433-1440.
131. S. R. Pauleta, I. Moura, in *Encyclopedia of Inorganic and Bioinorganic Chemistry*, Eds R.

- A. Scott, John Wiley & Sons, Ltd, New Jersey, **2017**.
132. J. Riester, W. G. Zumft, P. M. Kroneck, *Eur. J. Biochem.* **1989**, *178*(3), 751-762.
133. P. Wunsch, M. Herb, H. Wieland, U. M. Schiek, W. G. Zumft, *J. Bacteriol.* **2003**, *185*(3), 887-896.
134. W. G. Zumft, A. Viebrock-Sambale, C. Braun, *Eur. J. Biochem.* **1990**, *192*(3), 591-599.
135. W. G. Zumft, *J. Mol. Microbiol. Biotechnol.* **2005**, *10*(2-4), 154-166.
136. U. Honisch, W. G. Zumft, *J. Bacteriol.* **2003**, *185*(6), 1895-1902.
137. L. M. Taubner, M. A. McGuirl, D. M. Dooley, V. Copie, *Biochemistry* **2006**, *45*(40), 12240-12252.
138. M. A. McGuirl, J. A. Bollinger, N. Cosper, R. A. Scott, D. M. Dooley, *J. Biol. Inorg. Chem.* **2001**, *6*(2), 189-195.
139. L. M. Taubner, M. A. McGuirl, D. M. Dooley, V. Copie, *J. Biomol. NMR* **2004**, *29*(2), 211-212.
140. S. P. Bennett, M. J. Soriano-Laguna, Justin M. Bradley, D. A. Svistunenko, D. J. Richardson, A. J. Gates, N. E. Le Brun, *Chemical Science* **2019**, *10*(19), 4985-4993.
141. A. Dreusch, D. M. Burgisser, C. W. Heizmann, W. G. Zumft, *Biochim. Biophys. Acta* **1997**, *1319*(2-3), 311-318.
142. M. Giles, N. Morley, E. M. Baggs, T. J. Daniell, *Front. Microbiol.* **2012**, *3*, 407.
143. J. Simon, M. G. Klotz, *Biochim. Biophys. Acta* **2013**, *1827*(2), 114-135.

Table 1. The different oxidation states, spectroscopic data, and activities towards N₂O for the different forms of the CuZ center of N₂OR.

| “CuZ” form | Oxidation state (Cu _I – Cu _{IV} ligand) | Absorption maximum | Spin state | EPR | Turnover number (N ₂ O) | Ref. |
|--------------------------|--|--|---------------|---|--|---|
| CuZ(4Cu1S) | [1Cu ²⁺ :3Cu ¹⁺ :S:OH] (bridging OH ⁻) | 640 nm (~3.5 mM ⁻¹ cm ⁻¹) ^a | S=1/2 | $g_{\parallel} = 2.160, g_{\perp} = 2.040$ $A_{\parallel} = 6.1 \text{ mT}/A_{\perp} = 2.4 \text{ mT}^b$ | 0 | [93, 107, 108, 111, 113, 116, 122] |
| | [4Cu ¹⁺ :S] (empty) | No bands | S=0 | Silent | 321 s ⁻¹ | [90, 112, 119, 123, 124] |
| CuZ ⁰ (4Cu1S) | [1Cu ²⁺ :3Cu ¹⁺ :S:OH] (Cu _{IV} -OH ⁻) | 680 nm (~2.0 mM ⁻¹ cm ⁻¹) ^a | S=1/2 | $g_{\parallel} = 2.177, g_{\perp} = 2.05$ $A_{\parallel} = 4.2 \text{ mT}^c$ | 321 s ⁻¹ | [118, 121] |
| CuZ(4Cu2S) | [2Cu ²⁺ :2Cu ¹⁺ :2S] (bridging S ²⁻) | 545 nm (~5.0 mM ⁻¹ cm ⁻¹) ^a | S=0 | Silent | 0 | [90, 93, 116, 119] |
| | [1Cu ²⁺ :3Cu ¹⁺ :2S] (bridging SH ⁻) | 670 nm (~3.0-4.4 mM ⁻¹ cm ⁻¹) ^a | S=1/2 | $g_{\parallel} = 2.150, g_{\perp} = 2.035$ $A_{\parallel} = 5.6 \text{ mT}^d$ | 0.6 h ⁻¹ | [90, 93, 110, 116, 119, 123, 125, 126] |

N.D. – Not determined.

^aExtinction coefficients given per N₂OR monomer.

^bWith a 5:2 ratio.

^cConsidering two identical hyperfine coupling constants.

^dConsidering three identical ^{63,65}Cu hyperfine coupling constants.

Scheme and Figure Legends

Scheme 1 – Possible oxidation states of the CuZ core center. The oxidation states that have been observed and characterized for CuZ(4Cu1S) and CuZ(4Cu2S) are shaded in grey.

Figure 1. Major pathways of the nitrogen cycle. Different pathways are highlighted in different colors: denitrification blue, nitrification light brown, nitrogen fixation grey, anammox gold yellow, and dissimilatory nitrate reduction to ammonium (DNRA) green. The enzymes that catalyze each step are written above the corresponding arrow and the genes encoding the enzymes in denitrification, that is the major N₂O source, are written below the arrows. Figure adapted from [17, 142].

Figure 2. The canonical gene cluster and electron transfer pathway from the quinol/menaquinol pool to Clade I and Clade II N₂OR. Panel (A) shows the *nosZ* gene cluster organization of Clade I N₂OR and the proposed electron transfer pathway from NosR to a small electron donor protein (ED) that then transfers the electron to then CuA center of N₂OR. The possibility of a direct route from NosR to N₂OR is also represented. Panel (B) shows the *nosZ* gene cluster organization of Clade II N₂OR and the proposed electron transfer pathway from membrane-associated NosG/NosH to NosC2, then to NosC1 and finally to the *c*-type heme domain of *c*NosZ of *W. succinogenes*. Figure was prepared based on [77, 143]. PA = pseudoazurin, C = thioredoxin-like protein, *c* = *c*-type cytochrome, Fe/S = iron-sulfur cluster protein. The arrows in black correspond to hypothetical proteins, *dnr* - dissimilative nitrate respiration regulator, Q = quinone, MK = menaquinone.

Figure 3. Structure of Clade I *P. stutzeri* N₂OR functional homodimer. The backbone of one monomer is represented with the identified secondary structure colored in blue (N-terminal

domain) or light blue (C-terminal domain) with its transparent surface in light blue, and the other monomer is similarly represented in grey. CuA and CuZ centers are represented by spheres, in which the copper atoms are colored in blue. The distances between CuA and CuZ centers of the two monomers are given. Figure was prepared with Biovia Discovery Studio using PDB ID 3SBP for *P. stutzeri* N₂OR. Color scheme for the atoms: Cu in dark blue and S in yellow.

Figure 4. Structure of the different forms of CuZ center. **(A)** Coordination of CuZ(4Cu1S) in *P. denitrificans* N₂OR and **(B)** coordination of CuZ(4Cu2S) in *P. stutzeri* N₂OR. Figures were prepared with Biovia Discovery Studio using PDB ID 1FWX for *P. denitrificans* N₂OR and PDB ID 3SBP for *P. stutzeri* N₂OR. Color scheme for the atoms: carbon in grey, Cu in dark blue, N in light blue, S in yellow, O in red and I in violet.

Figure 5. Structure of CuZ center of *A. cycloclastes* N₂OR. **(A)** Coordination of iodide-bound CuZ(4Cu1S) and **(B)** of N₂O-bound CuZ(4Cu1S) (N₂O was modelled into the structure with data from [124]). Figures were prepared with Biovia Discovery Studio using PDB ID 2IWK for *A. cycloclastes* inhibitor-bound N₂OR and PDB ID 2IWF for *A. cycloclastes* N₂O-bound N₂OR. Color scheme for the atoms: carbon in grey, Cu in dark blue, N in light blue, S in yellow, O in red and I in violet.

Figure 6. Catalytic cycle of N₂O reduction by N₂OR with CuZ(4Cu1S). Intermediates 1 and 3 have been trapped and characterized, while intermediate 2 remains to be characterized. The scheme also shows the reduction of the [1Cu²⁺-3Cu¹⁺] oxidation state to [4Cu¹⁺] by reduced viologens (activation), which is not part of the catalytic cycle. Residues are numbered according to *P. denitrificans* N₂OR mature amino acid sequence. ED = electron donor.